

1
2 **PLYWOODS OF NORTHEAST ARGENTINIAN WOODS AND SOYBEAN**
3 **PROTEIN-BASED ADHESIVES: RELATIONSHIP BETWEEN**
4 **MORPHOLOGICAL ASPECTS OF VENEERS AND SHEAR STRENGTH**
5 **VALUES**

6 **E. S. Nicolao^{a1}, S. Monteoliva^{b2}, E. M. Ciannamea^{a3}, P. Stefani^{a4*}**

7
8 ^a National University of Mar del Plata, Research Institute of Materials Science and
9 Technology (INTEMA), National Scientific and Technical Research Council
10 (CONICET), Mar del Plata, Argentina.

11 ^b National University of La Plata, Agricultural and Forest Sciences Faculty, INFIVE-
12 CONICET Mar del Plata, Argentina.

13
14 ¹ <https://orcid.org/0000-0003-2549-953>

15 ² <https://orcid.org/0000-0002-8679-7633>

16 ³ <https://orcid.org/0000-0001-6982-1550>

17 ⁴ <https://orcid.org/0000-0002-8140-4415>

18
19 ***Corresponding author:** pmstefan@fi.mdp.edu.ar

20 **Received:** December 23, 2020

21 **Accepted:** September 21, 2021

22 **Posted online:** September 21, 2021

23 **ABSTRACT**

24 Three-ply plywoods were produced using pine and *Eucalyptus* northeast Argentinian
25 woods. A no-added formaldehyde biobased-adhesive was used for assembly, based on
26 chemically modified soy protein concentrate. In this work we focused on the relationship
27 between bonding quality parameters of the plywoods and the morphology of the glued
28 line. Wood characteristics such as contact angle, roughness, density and moisture content
29 were measured prior to plywood assembly. Bonding quality parameters (percentage of
30 wood failure and shear strength) of the plywood were measured according to Argentinean
31 standard IRAM 9562 and the results were evaluated with respect to microscopic
32 observations of the glue joint. *Eucalyptus* wood was suitable for plywood interior
33 condition applications, while pine barely exceeded the standards imposed by the norm.

34
35 **Keywords:** Biogenic adhesive, bonding quality, mechanical properties, plywood, wood
36 taxonomy.

38 **1. INTRODUCTION**

39 Increased demand of natural resources, mostly wood, have led to the development of new
40 alternative materials for countless industrial applications. In particular, veneer-based
41 products, especially plywoods, which are mostly used for structural applications, are
42 important due to their versatile use and lower cost in comparison to other composite
43 materials (Buddi *et al.* 2017). According to FAO data, the world production of veneer
44 sheets and plywood in 2018 was 163 million m³ and it is expected to rise in the following
45 years (FAO 2018).

46 The following work focuses especially on *Eucalyptus* (EU) and pine (PI) plywoods using
47 a soy protein concentrate (SPC) based adhesive for the following reasons.

48 Argentina's forest resource is made up of both exotic and native species. Current
49 environmental policies and regulations linked to the preservation of natural forests and
50 the increasing demand for wood and its derivatives, have promoted the sustainable
51 production of cultivated forest. There are approximately 1180000 hectares of cultivated
52 forests of PI and EU species, 25 % corresponding to EU concentrating in the
53 Mesopotamia area of Argentina, which ensures the local availability of resources
54 (Nicolao *et al.* 2020). Furthermore, the forestry sector can still be explored if its full
55 potential is taken into account (Pizzi 2006).

56 Anatomically, differences between species are related to cell structure: that is the types,
57 sizes, ratios between cell walls and lumens width, pits, and arrangements of different cells
58 that comprise the wood. These differences make woods heavy or light, stiff or flexible,
59 hard or soft (Piter *et al.* 2007, Nordqvist *et al.* 2013).

60 The structure of softwoods is relatively simple compared to hardwoods. The axial or
61 vertical system is composed mostly (95 % - 98 %) of axial tracheids for water conduction
62 and mechanical support. Hardwoods, on the other hand, have perforated tracheary

63 elements (vessels elements) for water conduction (10 % - 20 %), fibres (60 % - 70 %) for
64 mechanical support and parenchyma (5 % - 10 %), as part of the axial system (Frihart
65 2010).

66 Moreover, its structure not only depends on the specie being analyzed (hardwood or
67 softwood in large terms) but also depends on subtler characteristics, such as percent of
68 early or late wood within the tree-ring in the growing season, which gives variations in
69 the ratio between the width of the lumen and the thickness of the cell wall (Bulfe and
70 Fernandez 2017). Changes from early to late wood may be more or less subtle within in
71 the same ring depending the specie, noticing that these change are important for pine
72 (Denne 1989), and not for *Eucalyptus* wood. Understanding all this differences in cellular
73 architecture allows insight to the realm of wood as an engineering material.

74 Wood is composed of cellulose, lignin, hemicelluloses, and minor amounts (usually less
75 than 10 %) of extractives materials contained in a cellular structure.

76 Alternative adhesives have emerged to contrast the negative effects of urea-
77 formaldehyde, the main adhesive used in wood composite materials, since formaldehyde
78 has been classified as a human carcinogen and is obtained from non-renewable resources
79 (Ghahri *et al.* 2021). Regulations on formaldehyde emissions (Salthammer *et al.* 2010)
80 have become a driving force towards the search of new adhesive formulations based on
81 sustainable raw materials such as starch, natural polyphenols, carbohydrates and proteins
82 (Pizzi 2006; Frihart and Birkeland 2014). Numerous works have been done so far with
83 respect to natural adhesives including protein (Mo and Sun 2013, Nordqvist *et al.* 2013),
84 tannin (Stefani *et al.* 2008, Xi *et al.* 2020), tamarind (Buddi *et al.* 2017), and lignin-based
85 adhesives (Ang *et al.* 2019) to name some of them. In particular, soy-based adhesives are
86 a promising alternative. They are produced from renewable agricultural resources, are
87 environmentally friendly and are less likely to cause health problems (Nicolao *et al.*

88 2020). Argentina is the third largest producer of soybeans in the world (54 million tones
89 2019/2020) (ASA 2020), so the use of adhesives based on this crop is also attractive from
90 the point of view of taking advantage of the own country's resources. Our research group
91 has made numerous studies in this field, involving from the development of soy protein
92 concentrate (SPC) based adhesives to its application in plywood and rice husk based
93 boards (Ciannamea *et al.* 2010, Ciannamea *et al.* 2012, Ciannamea *et al.* 2017, Nicolao
94 *et al.* 2020). According to our previous research, particleboards based on rice husk and
95 SPC treated with boric acid showed the best mechanical and water resistance properties,
96 in comparison with other studied chemical treatments, as urea, citric acid or alkali
97 (Ciannamea *et al.* 2012, Chalapud *et al.* 2020). Boric acid can react with OH from side
98 groups of proteins, carbohydrates in soybean concentrate and BSPC can also react with
99 OH groups present in wood, favored by hot pressing conditions (Ciannamea *et al.* 2012).
100 In addition to all the possible variations in wood structure named above, plywoods are
101 materials that involve joints between veneer faces. These joints provide even more
102 discontinuities in the material that must be studied and paid attention to. Joints under load
103 must transfer stress from component to component through the interphase region, thus,
104 the characteristics of the bond will impact on the performance of the plywood (Kamke
105 and Lee 2007, Piter *et al.* 2007). Making a chain-link analogy of a union between woods,
106 the bond will be as good as the weakest link in the chain (Marra 1992). An expected
107 plywood performance would be that in which the weakest link is located inside the wood
108 meaning that mechanical performance should be limited by wood resistance and not by
109 the adhesion itself. Thus, one of the standards used in plywood manufacture, IRAM 9562
110 (2007), establishes not only shear strength tolerances but also wood failure percentage
111 tolerances (WF %) as a quality criteria.

112 Several adhesion models, with their focus on surface interactions between the adhesive
113 and the adherent, have been proposed over the years for most adherents; however, they
114 have failed when applied to wood composites mainly due to wood variability explained
115 before (Jakes *et al.* 2019). Numerous studies have focused on understanding what
116 happens at the interface between plywood veneers (Chandler *et al.* 2005, Frihart 2005,
117 Piter *et al.* 2007, Jakes *et al.* 2019). Understanding the differences between the species
118 used, in morphological and morphometric terms, allows predicting, in a certain way, the
119 behavior of a glued joint.

120 In this work we employed a previously developed no-added formaldehyde adhesive based
121 on chemically treated SPC to obtained EU and PI plywoods. We specially focused in the
122 relationship between bonding quality parameters of the plywoods (measured according
123 to IRAM 9562 standard) and the microscopic observations of the glued joints. It is
124 expected that the morphology/morphometry of each one of the species used and the
125 degree of penetration of the adhesive plays a fundamental role in the quality of the gluing.

126 **2. MATERIALS AND METHODS**

127 **2.1. Materials**

128 Soybean protein concentrate (SPC, Solcom S 110) was provided by Cordis SA (Villa
129 Luzuriaga, Buenos Aires, Argentina). SPC presented 7 % moisture, 69 % protein, 1 %
130 fat, 3 % fibers, 5 % ash and about 15 % non-starch polysaccharides (mainly cellulose,
131 non cellulose polymers and pectin polysaccharides) as mean composition and has an
132 average particle size that could pass through a 100 mesh. Veneers of EU (*Eucalyptus*
133 *grandis*) and PI (*Pinus taeda*), from specimens cultivated in northeast region of
134 Argentina, were supplied by Forestadora Tapebicua SA. The age of the PI veneer's logs
135 was 19 years, while for EU it was only 12 years old. Veneers were carefully inspected
136 and selected avoiding major defects such as knots or cracks. Sodium hydroxide (NaOH,

137 Anedra, Argentina), diiodomethane, Glycerol (Anedra, Argentina, 99 % purity) and
138 safranin were purchased from the Sigma Chemical Co. (St. Louis, MO).

139

140 **2.2. Methods**

141 **2.2.1. Adhesive preparation**

142 Adhesive was prepared according previous works (Ciannamea *et al.* 2012) by dispersing
143 SPC in a 0,3 % w/v boric acid (BA) solution at a ratio 1:10 (SPC:BA solution) under
144 stirring ($500 \text{ rad}\cdot\text{s}^{-1}$) at room temperature for 2 h. The adhesive was lyophilized for 72
145 hours and stored in a dry environment for later use (BSPC stands boric modified SPC).

146

147 **2.2.2. Rheological study of the adhesive**

148 The apparent viscosity of the SPC-based adhesives was measured with an Anton Paar
149 MCR 301 rheometer (Graz, Austria) at $25 \text{ }^\circ\text{C} \pm 0,2 \text{ }^\circ\text{C}$ over a shear rate range of 1 s^{-1} to
150 750 s^{-1} . Lyophilized adhesives were dispersed in distilled water in weight relations of 1:4,
151 1:5, 1:6, 1:7 and 1:10 (lyophilized BSPC adhesive:water ratio), mixed for 10 min, and
152 transferred into the sample holder of the viscometer.

153

154 **2.2.3. Veneers and plywoods preconditioning**

155 EU and PI veneers, as well as plywoods, were kept 7 days in an environmental chamber
156 at $65 \% \pm 5 \%$ relative humidity and $20 \text{ }^\circ\text{C} \pm 2 \text{ }^\circ\text{C}$ before carrying out any test. All veneers
157 samples were sanded within 24 hours before any test or plywood assembly with an
158 abrasive paper until achieving an average surface roughness R_a of $7 \text{ } \mu\text{m} \pm 2 \text{ } \mu\text{m}$.

159

160 **2.2.4. Veneer characterization**

161 **2.2.4.1. Density and humidity**

162 Density of veneers was determined following norm IRAM 9544 on samples previously
163 stabilized in environmental chamber. Weight was measured gravimetrically using an
164 analytical balance (Ohaus, $\pm 0,0001$). The dimension of the testing samples was measured
165 with a digital caliper (Asimeto model 307-06-4, Germany, 0-150 mm $\pm 0,01$ mm) and
166 thickness was measured using a digital micrometer (Asimeto model IP65, Germany, 0-
167 25 mm $\pm 0,01$ mm) at eight random locations of each specimen.
168 The same samples were dried at 102 °C ± 3 °C to constant weight in a convection oven
169 in order to calculate moisture content according to IRAM 9532.

170

171 **2.2.4.2. Surface energy and contact angle**

172 The free surface energy was calculated by means of Owens–Wendt method. Following
173 the description reported by Vazquez et al (Vázquez *et al.* 2011), it is possible to calculate
174 the polar and dispersive components of the surface energy by means of the equation (1):

$$175 \frac{0.5\gamma_{LV}(1+\cos\theta)}{\sqrt{\gamma_{LV}^d}} = \sqrt{\gamma_{SV}^p} * \left(\frac{\gamma_{LV}^p}{\gamma_{LV}^d}\right)^{\frac{1}{2}} + \sqrt{\gamma_{SV}^d} \quad (1)$$

176 Where θ the contact angle formed between the liquid and the solid and γ_{LV}^p and γ_{LV}^d are
177 the polar and dispersive components of the solid's free surface respectively. Linearizing
178 equation 1, energy can be obtained as the slope and ordinate at the origin, respectively,
179 whose sum results in the total value of the free surface energy.

180 The polar component γ_{LV}^p and dispersive component γ_{LV}^d of each of the liquids used are
181 well known values reported in literature (Scheickl and Dunky 1998; Vázquez *et al.* 2011).

182 These liquids are: distilled water ($\gamma_{LV}^p=51$ mN·m⁻¹, $\gamma_{LV}^d=21,8$ mN·m⁻¹), glycerol ($\gamma_{LV}^p=30$
183 mN·m⁻¹, $\gamma_{LV}^d=34$ m·Nm⁻¹) and diiodomethane ($\gamma_{LV}^p=0$ mN·m⁻¹, $\gamma_{LV}^d=50,8$ mN·m⁻¹). θ Is
184 calculated by means of the following approach. The wetting process can be divided into
185 two wetting phases: an extension phase in which the wetting speed ($d\theta / dt$) is relatively

186 fast and a penetration stage, in which the rate of change of the contact angle is almost
187 constant (Wolkenhauer *et al.* 2009, Vázquez *et al.* 2011). Equilibrium contact angle θ is
188 considered at the point where $d\theta / dt$ becomes constant.

189 Ten measurements were made in PI and EU samples employing a 7 μl drop.
190 Measurements were made perpendicular to the direction of the wood fibers. A Rame-Hart
191 contact angle goniometer equipment (New Jersey, USA) was used which can record 15
192 images $\cdot\text{s}^{-1}$.

193 **2.2.4.3. Roughness**

194 Surface roughness of EU and PI veneer samples were measured using a portable Handsurf
195 profilometer (Accretech, Japan) unit consisting of main unit and pick-up. The stylus
196 traverses the surface at a constant speed of 1,0 $\text{mm}\cdot\text{s}^{-1}$ over 12,5 mm. A total of 12
197 measurements evenly distributed were taken from the surface of each sample for Ra
198 roughness measurements.

200 **2.2.5. Plywood assembly**

201 EU and PI veneers with an average thickness of 2,70 $\text{mm} \pm 0,07 \text{ mm}$ and 2,90 $\text{mm} \pm 0,7$
202 mm , respectively, were carefully inspected and selected taking into account a uniform
203 thickness, uniform surface and absence of wood defects, such as knots, cracks or
204 imperfections caused by veneer machinery.

205 The lyophilized BSPC adhesive was dispersed in distilled water in 1: 6 and 1: 7 weight
206 ratios and stirred for 10 minutes at 500 $\text{rad}\cdot\text{s}^{-1}$ at room temperature. A blue commercial
207 food colorant was added to clearly distinguish the adhesive on wood surfaces.

208 Three ply plywoods were obtained with both woods, *Eucalyptus* and pine, using spread
209 rates of 311 g/m^2 and 355 g/m^2 of wet adhesive in double glue line, with BSPC:water
210 mass ratio 1:6 and 1:7, respectively (Liu and Li 2002). Pre-assembling time was 20

211 minutes. Hot press time, temperature and pressure were adjusted to 10 min, 140 °C and
212 1,5 MPa, respectively. Three samples of each conditions were made: *Eucalyptus* with 1:6
213 BSPC:water dispersion (EU 1:6), *Eucalyptus* with 1:7 BSPC:water dispersion (EU 1:7),
214 pine with 1:6 BSPC:water dispersion (PI 1:6) and pine with 1:7 BSPC:water dispersion
215 (PI 1:7). Each plywood was cut in 20 test specimens according to Argentinian norm
216 IRAM 9562.

217 **2.2.6. Plywood bond quality analysis**

218 Plywoods bond quality analysis was measured according to Argentinian norm IRAM
219 9562. Test samples were divided into two groups, group A: samples without immersion
220 treatment and group B: samples subject to a 24-hour water immersion treatment at room
221 temperature.

222 Wood failure percentage was analyzed using an image software Image Pro (Media
223 Cybernetics, USA).

224

225 **2.2.7. Bond microanalysis**

226 Microsections with a thickness of 30 um to 35 um were prepared from EU and PI
227 plywoods after shear strength test, using a microtome. The area of interest for the
228 microsections was that located between the two notches and the plane of sectioning was
229 oriented parallel to the edge of the probe. The micro sections were taken in such way that
230 they could show two successive wood veneers and the bond line between. Sections were
231 stained with safranin (1 % v/v) and mounted into a microscope slice. Digital images were
232 taken under a light microscope (Olympus CX31, Japan) attached to a digital camera
233 (Infinity Lumenera, Canada). The images were then processed through specific software
234 (ImagePro, Media Cybernetics, USA).

235

236 **2.3. Statistical analysis**

237 Experimental data were statistically analyzed using the one-way analysis of variance
238 (ANOVA) along with Tukey's tests at 95 % confidence interval ($\alpha=0,05$).

239

240 **3. RESULTS AND DISCUSSION**

241 **3.1. Rheological analysis of dispersed BSPC**

242 The rheological behavior of BSPC with different water ratios was studied. Lyophilized
243 adhesive was re-dispersed in distilled water in 1:10, 1:7, 1:6, 1:5, 1:4 ratios. Viscosity
244 curves of all BSPC-based adhesives (Fig. 2) follow a classic shear-thinning behavior
245 (viscosity decreasing with increasing shear rate) as reported by Ciannamea *et al*
246 Ciannamea *et al.* 2012). As expected, viscosities were higher in more concentrated
247 dilutions, being much higher in 1:4 dispersions than the rest of them (two orders of
248 magnitude higher than 1:5 dispersions). The apparent viscosity at low shear rate ($1s^{-1}$ at
249 $25\text{ }^{\circ}C$) of 1:10, 1:7, 1:6, 1:5 and 1:4 ratios was 5,25; 10,4; 35,9; 148 and 2400 Pa.s,
250 respectively. There are three factors that an adhesive need to fulfill to form a proper bond:
251 it must wet the surface, flow over and penetrate into the substrate without losing the
252 adhesiveness between particles. An optimum penetration into the wood is considered
253 essential for a good bond formation and this is partially dependent on the viscosity of the
254 adhesive (Ciannamea *et al.* 2010). Adhesives must be fluid enough to flow into the
255 microscopic holes, or capillary structure, of wood, but without causing over penetration.
256 Tests carried out, concluded that adhesives with viscosities 1: 4 and 1:5 were not feasible
257 from a practical point of view, in accordance with Kumar et al (Kumar *et al.* 2002). High
258 viscosity dispersions resulted too viscous to apply in veneers surfaces, resulting in
259 insufficient penetration that can cause minimal surface contact for chemical bonding or
260 “mechanical interlocking” (Chandler *et al.* 2005). On the other hand, test carried on with

261 1:10 dispersions resulted in too dilute to be applied on veneer's faces, producing over
262 penetration. Therefore, dispersions of 1:6 and 1:7 were chosen to work with in further
263 experiments.

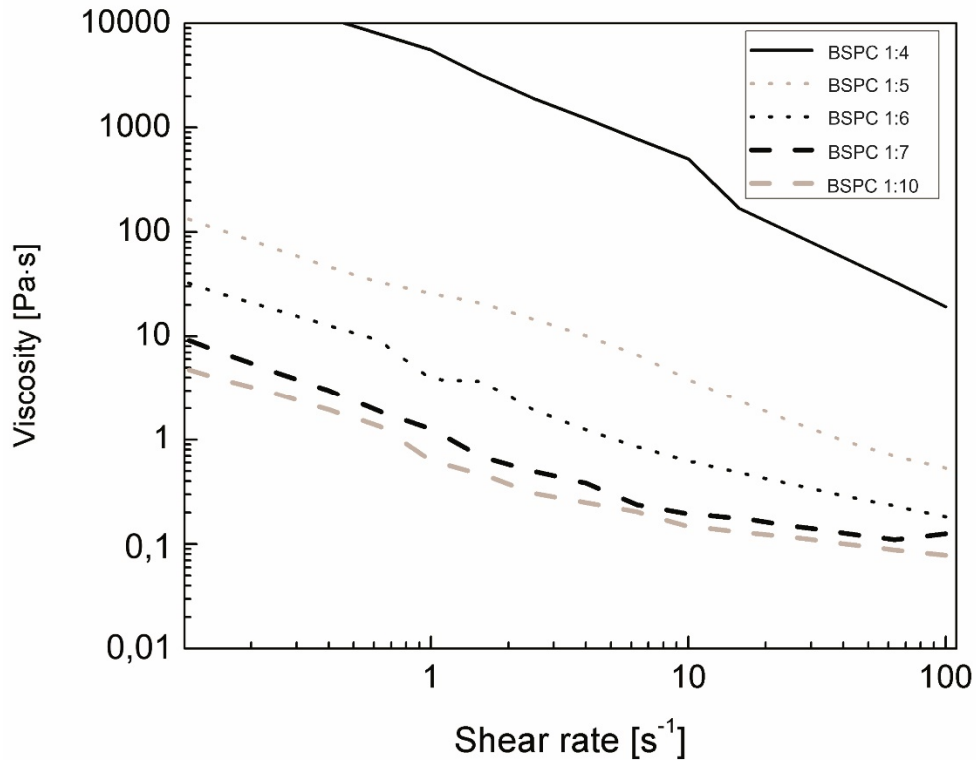


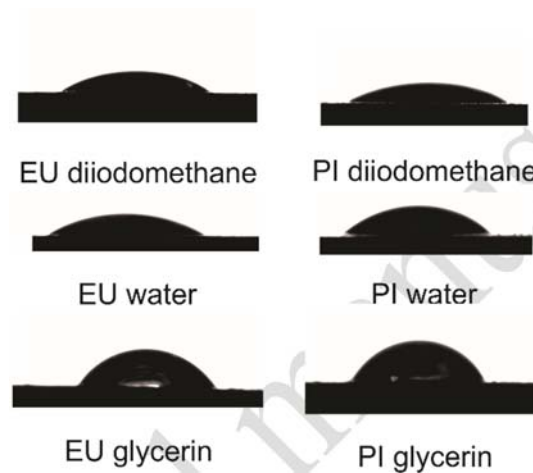
Figure 1: Viscosity as function of shear stress of soy bean adhesives.

264 3.2. Woods characterization

265 Density is a parameter that, apart from varying between species, varies within the same
266 species and even within the same specimen (Calvo *et al.* 2006; Goche Télles *et al.* 2011).
267 Both species show a great variation in wood density depending on the age of the trunk,
268 being greater the older the specimen (Sánchez Acosta *et al.* 2005). For species of the same
269 age, average density of UE is higher than the PI density.

270 The density of the *Eucalyptus* veneers was $0,54 \text{ g}\cdot\text{cm}^{-3} \pm 0,10 \text{ g}\cdot\text{cm}^{-3}$ with a moisture
271 content of $9,4 \% \pm 0,15 \%$. Pine veneers presented a density of $0,52 \text{ g}\cdot\text{cm}^{-3} \pm 0,09$

272 $\text{g}\cdot\text{cm}^{-3}$ with a moisture content of $8,6\% \pm 0,5\%$. The young age of the EU veneers,
 273 relative to the age of the PI veneers, may explain the low density in them and therefore
 274 the narrow range of densities between the two species.
 275 Contact angle was measured for PI and EU using three different liquids which differ in
 276 polarity: diiodomethane, distilled water and glycerol. Figure 2 shows the equilibrium
 277 contact angle for PI and EU, while Table 1 shows the results of equilibrium contact angle
 278 and surface energies.



279

280

Figure 2: Equilibrium contact angle for (left) *Eucalyptus* and (right) pine.

281

Table 1: Surface energies and equilibrium contact angles for PI and EU.

WOOD	γ	γ^d	γ^p	θ_{water}	$\theta_{\text{diiodomethane}}$	θ_{glycerin}
	[$\text{mJ}\cdot\text{m}^{-2}$]					
PI	53,3	33,0	20,3	39 ± 3	34 ± 1	63 ± 7
EU	54,6	30,6	24,0	30 ± 3	35 ± 5	66 ± 7

282

283 During the initial phases of spreading and soaking of the drops, the change in contact
 284 angle was faster, getting slower towards the end of the process. A significant difference
 285 in the time necessary for the complete soaking of the drop could be seen between the
 286 solvents used, being quicker for diiodomethane, water, and the least for glycerin which

287 can be related to increasing viscosity. Regardless PI or EU, equilibrium contact angles
288 were higher for glycerin and no significant differences ($p > 0,05$) were found between
289 diiodomethane and water equilibrium contact angles. Moreover, angles were no
290 significant different between woods. Surface energies for PI and EU were also similar,
291 being $53,3 \text{ mJ}\cdot\text{m}^{-2}$ for PI and slightly higher, $54,6 \text{ mJ}\cdot\text{m}^{-2}$, for EU.

292 The similarity between contact angle of PI and EU may be attributed to numerous reasons.
293 In the first place the measurements were made in the tangential plane, perpendicular to
294 the fiber's direction. Previous studies show greater variations in contact angle
295 measurements in the radial plane where radial cells are expose to the surface (Scheikl and
296 Dunky 1998). Moreover, contact angles strongly depend on surface roughness (Papp and
297 Csiha 2017) and in less amount among other parameters such as wood moisture, density
298 and presence of extractives (Boehme and Hora 1996). Besides similar densities, both
299 woods presented similar roughness, plus preconditioning moisture and temperature
300 variables were the same for both. This explains the low differences in contact angles
301 shown in table 1.

302 Low water contact angles indicate a good wettability for both EU and PI with the SPC
303 based adhesive (Aydin and Colakoglu 2007). From these results it is expected a good
304 affinity between the adhesive and both woods, EU and PI. Therefore, any difference in
305 the mechanical behavior between EU and PI plywoods may be attributable to morphology
306 differences, rather than to affinity between wood and adhesive.

307 **3.3. Bond quality analysis**

308 The properties of the plywood were evaluated in terms of the bond quality test according
309 to standard norm IRAM 9562. Tests were carried out both under dry conditions and after
310 24 hours of immersion in water at $20 \text{ }^\circ\text{C} \pm 3 \text{ }^\circ\text{C}$ (class 1: suitable for dry interior use).
311 Besides the shear strength expressed in $\text{N}\cdot\text{mm}^{-2}$, another parameter that defines the quality

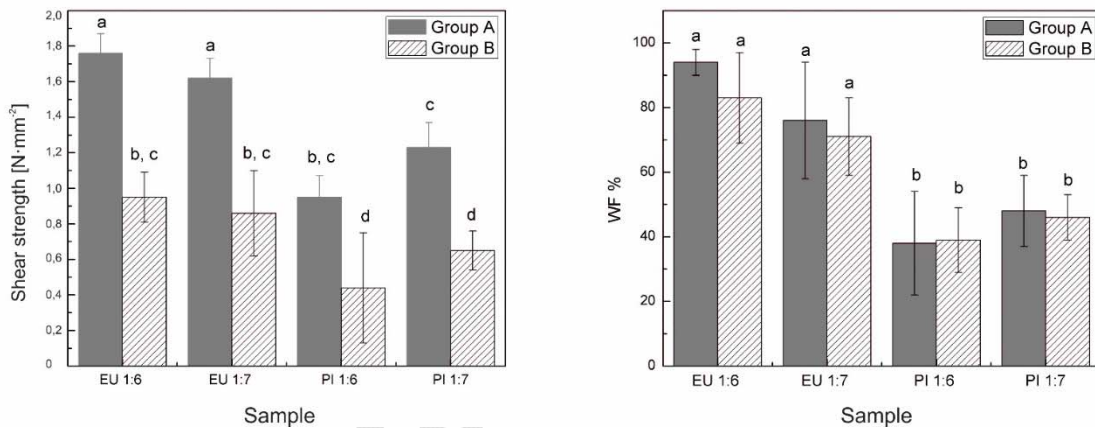
312 of the bond is the percentage of wood fiber failure (WF %). A complete wood failure (100
313 % of wood fracture surface) indicates an excellent adhesion between veneers, which
314 means that the measured strength is mainly determined by the strength of wood and not
315 weakened by the presence of the joints between veneers. According to IRAM 9562, WF
316 % values are determined visually by comparing with reference illustrations that show
317 different percentages of wood failure. However, often it is not easy to visually estimate
318 WF % values because with certain combinations of wood and adhesive, the wood failure
319 area can only be detected in texture and generally requires a specific training (Plinke). In
320 order to clearly distinguish the fracture mode, a blue colorant was added to the adhesive
321 which helps to identify the presence of adhesive in the fracture zone. In addition, an image
322 processing software was used to detect, differentiate and measure the areas of adhesive
323 and wood and determine the WF % with greater precision. Figure 3 shows the differences
324 in fracture behavior of both PI and EU.



325
326 **Figure 3:** Fracture surface analysis. **(Left)** *Eucalyptus* and **(Right)** pine where the blue
327 area corresponds to the exposed glued line.
328

329 Figure 4 shows the comparison of shear strength and WF % values under dry (group A)
330 and wet conditions (group B). In all four cases, shear strength values decreased by at least
331 40 % after 24 h immersion. Wang et al. reported similar behavior when testing poplar and

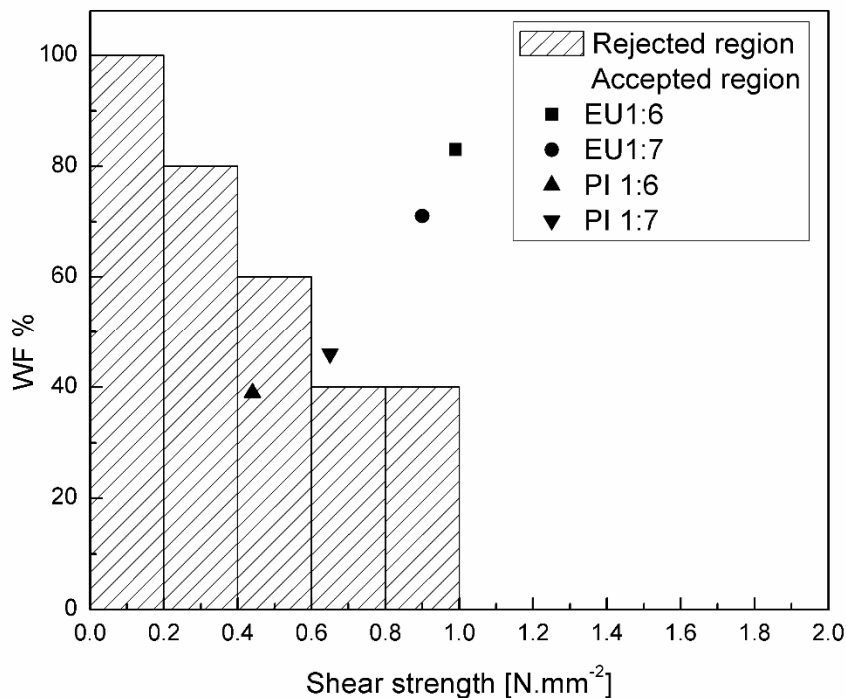
332 *Eucalyptus* veneers: shear strength of $0,82 \text{ N}\cdot\text{mm}^{-2} \pm 0,07 \text{ N}\cdot\text{mm}^{-2}$ had been reduced to
333 $0,44 \text{ N}\cdot\text{mm}^{-2} \pm 0,08 \text{ N}\cdot\text{mm}^{-2}$ after immersion in water at $63 \text{ }^\circ\text{C}$ for 3 h (Wang *et al.* 2018).
334 No significant differences between 1:6 and 1:7 dispersions could be seen for PI and EU
335 under dry conditions. PI 1:7 shear strength values in dry conditions were not significant
336 different ($p < 0.05$) from EU samples tested in humid conditions evidencing the poor
337 quality of PI unions with respect to EU ones. 1:6 PI values were even lower than 1:7 PI
338 values. It is interesting to notice that WF % results are not susceptible to moisture content
339 and adhesive solid content as there are no significant differences within EU probes and
340 within PI samples (Figure 4 right).



341 **Figure 4:** Comparison between A condition (dry) and B condition (wet) samples: **(left)**
342 shear strength values (shear strength), **(right)** wood failure percentage values (WF %).
343 Bars followed by different letters are significantly different ($p < 0,05$) by Tukey's Test.
344

345 IRAM 9562 standard establishes tolerance limits of WF % depending on the values of
346 shear strength achieved. For example, if shear strength exceeds values of $1 \text{ N}\cdot\text{mm}^{-2}$, there
347 are no restrictions in values of WF %. As shear strength values become lower, the
348 proposed WF% limits become increasingly strict. In this way a shear strength vs. WF %
349 graph is divided into an acceptable zone and a rejected zone as seen in Figure 6. Results
350 of shear strength and WF % condition B samples are also shown in Figure 5. EU plywoods
351 exhibit shear strength and WF % values around $1 \text{ N}\cdot\text{mm}^{-2}$ and over 70 %, respectively,
352 being significantly higher than PI values. Results revealed better properties using 1:7

353 dispersions than 1:6 for EU and that both conditions were within the accepted region of
354 the graph. Regarding PI results, the properties are significantly lower than EU, with PI
355 1:6 samples not accepted due to the qualities established in IRAM 9562 and PI 1:7 very
356 close to the rejected region plus no significant differences were shown between them.



357

358 **Figure 5:** Relationship between wood failure percentage values (WF %) and shear
359 strength for B condition samples (wet).

360

361 3.4. Bond line microscope analysis

362 This section intends to establish a relationship between the morphological and

363 morphometric characteristics of each wood species used and the experimental response

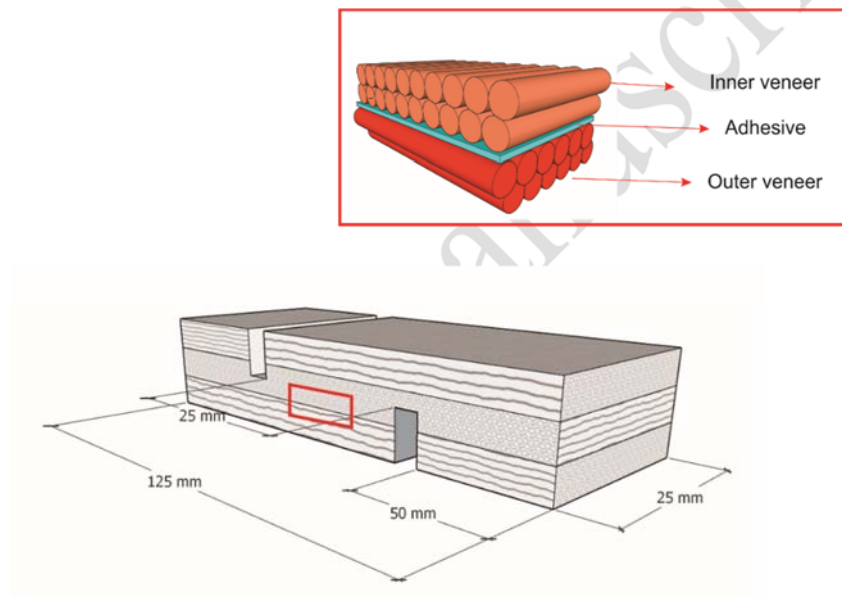
364 exposed above. The wood has mainly two cell systems, the axial and the radial system.

365 The axial system has cells or rows of cells with their major axes oriented vertically, that

366 is, parallel to the main axis of the trunk, while the radial system is formed by cells oriented

367 horizontally in relation to the axis of the trunk. Each of these systems reveals an aspect

368 of the wood morphology according to the type of cut being made: radial, tangential and
369 transverse (Rowell 2012). In this study, when making a cross-section along the edge of
370 the probe (between the notches), the inner veneer cells are cut in a radial plane and their
371 smallest dimensions can be seen as shown in figure 6. It should be noted that the adhesive
372 penetration study was only carried out on the central face of the plywood since its fibers
373 are oriented perpendicular to the direction of application of the force, being the veneer
374 most prone to fail. In fact, the IRAM 9562 test is designed in such a way that the failure
375 occurs through it.



376

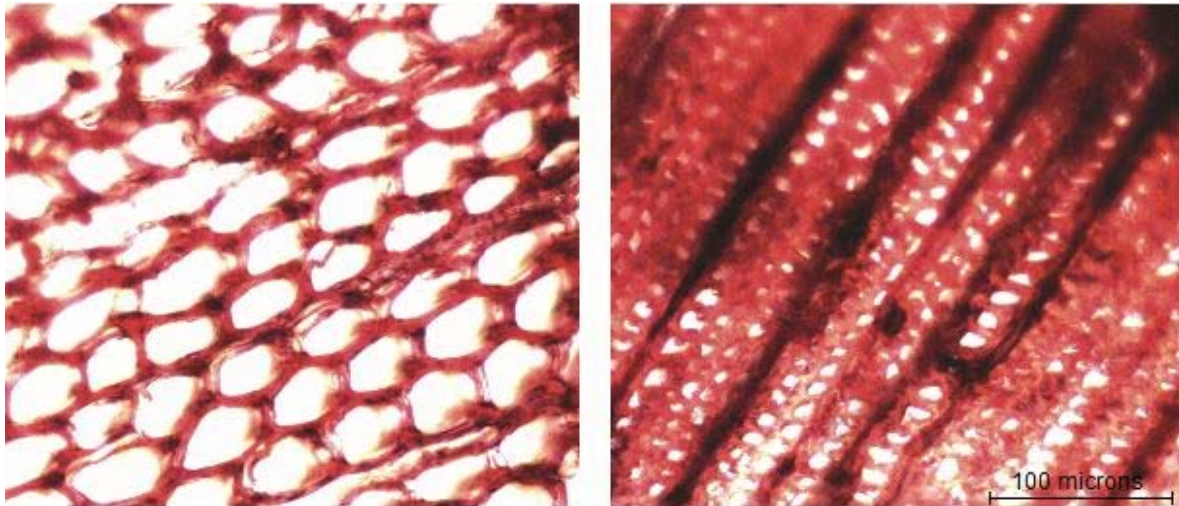
377 **Figure 6:** Scheme of IRAM 9562 samples dimensions and microsectioning area
378 of bondline.

379

380 In this way, it is possible to see (and measure) characteristics such as the diameter of
381 fibers, vessels, tracheid, parenchyma cells, vessel frequency, vessel area and vessels
382 distribution among others, depending on whether it is PI or EU specie (Frihart and Hunt
383 2010). The single most important distinction between the two general kinds of wood is
384 that EU (hardwood) have a characteristic type of cells call vessel elements (or pore)
385 whereas PI (softwood) only presents tracheid in their axial system. These cells type have
386 very different morphometry (diameter and length). The strength and quality of the union

387 is expected to be intrinsically correlated to the way and degree of penetration of the
388 adhesive in these different morphologies (de Oliveira *et al.* 2020).

389 Figure 7 shows images 100x of both PI and EU morphological aspects of each type of
390 wood axial system.
391

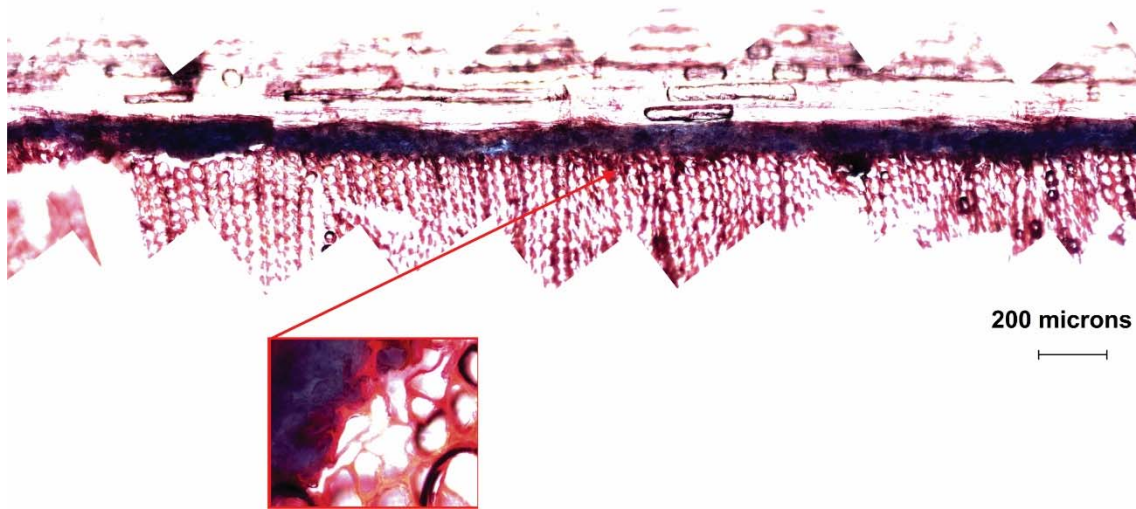


392
393 **Figure 7:** 100x wood images. Transverse section of earlywood tracheids (**Left**) pine
394 and (**right**) *Eucalyptus* fibers.

395 EU fiber lumen diameter average was $13 \mu\text{m} \pm 4 \mu\text{m}$, in accordance with Monteoliva *et*.
396 *al* measurements for *Eucalyptus grandis* species of Argentina (Monteoliva *et al.* 2015).
397 PI earlywood lumen average was $26 \mu\text{m} \pm 7 \mu\text{m}$. The greatest difference between both
398 cell structures is in the relationship between the width of the cell wall and the diameter of
399 the lumen, being greater in the earlywood tracheids, making them more likely to be
400 crushed and weakened by unwinding processes or pressing stages than *Eucalyptus* fibers,
401 or at least the damage is greater. In addition, when aqueous adhesives are used, the cells
402 close to the glue line can reach a high moisture content. In these conditions these cells,
403 especially in earlywood, are more likely to buckle during pressing (Hunt et al 2018).

404 Figure 8 shows the bondline of a PI sample and the deformation or rupture of earlywood
405 tracheids next to the bondline. Broken or crushed in the surface cells might increase the

406 potentiality of failure through the bondline in PI samples and it might be one reason for
407 the difference in WF % values between PI and EU presented in the previous section.

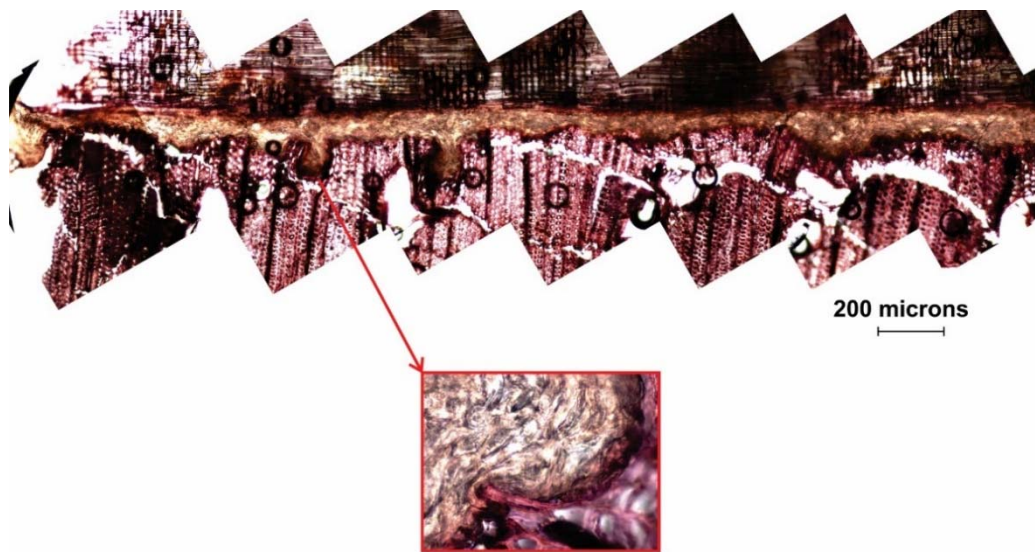


408

409 **Figure 8:** Tracheids deformation close to the bondline in PI samples.

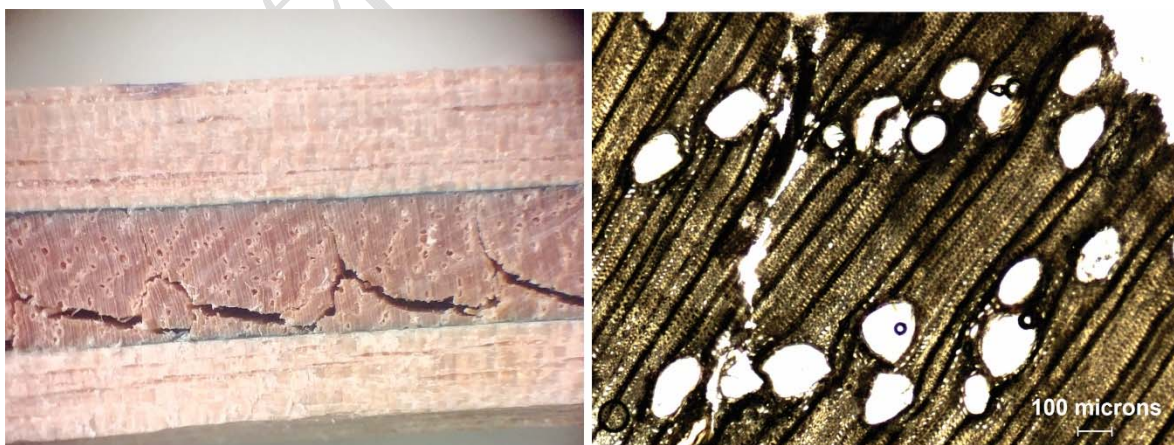
410 It is known that the presence of vessels weakens the strength of wood. However, the
411 vessels present in EU that are exposed to the veneers surface are filled with adhesive and
412 act as points where mechanical interlocking is enhanced providing additional shear
413 strength (Frihart 2005). Moreover, the surface contact area between the adhesive and the
414 cell wall increases considerable at these points (vessels). Contact area is directly related
415 to adhesion force due to covalent bonding and formation of secondary chemical bonds
416 increasing resistance to debonding (Kamke and Lee 2007). At these points, the average
417 thickness of the glue line increases by almost 200 % as can be seen in Figure 9. On the
418 contrary, the unfilled vessels located within the central part of plywood are weak zones
419 prone to break under shear stress load. It is worth noting the absence of tylose and
420 deposits in this *Eucalyptus* vessels which could partially or completely block the vessel
421 lumen.

422



423 **Figure 9:** *Eucalyptus* bond line. Vessels filled with adhesive act as mechanical
424 interlocking and contact area between adhesive and wood is increased.
425

426 Also, by analyzing the samples's cross-sectional profile, it can be seen that the fracture
427 extends with a constant profile across the entire width of the sample, as reported by other
428 authors for birch plywood samples particularly when tested with lathe checks pulled
429 closed (Rohumaa *et al.* 2013, Hunt *et al.* 2018). The latter could be related not only to the
430 presence of lathe checks but also to the diagonal arrangement of the vessels oriented 45°
431 with respect to the load as it is shown in Figure 10.



432
433 **Figure 10: (left)** Serrate profile fracture in EU wood (macroscopic image 10x) and
434 **(right)** empty EU vessels with diagonal pattern from interior of plywood (microscopic
435 image 40x).
436

437 4. CONCLUSIONS

- 438 • The performance of the biobased BSPC adhesive was excellent for *Eucalyptus*
439 plywood accomplishing IRAM 9562 standards for interior use class I. No
440 significant differences were found between 1:6 and 1:7 dispersions.
- 441 • PI plywoods showed low values of shear strength and %WF. 1:7 adhesive
442 dispersion barely accomplishing norm IRAM 9562 while 1:6 dispersion failed
443 it.
- 444 • A relationship could be established between the WF% values and the
445 morphological aspect of each type of wood. Broken or crushed tracheids in
446 pine enhance debonding between veneers giving lower values of WF%,
447 whereas the presence and diagonal arrangement of vessels in EU wood can act
448 as weak links contributing to determine the path of fracture propagation
449 through the central veneer.

451 ACKNOWLEDGEMENTS

452 The authors acknowledge the financial support from CONICET (National Scientific and
453 Technical Research Council) and National Agency of Promotion of Science and
454 Technology (ANPCyT) grand number PICT 2016-0445.

456 5. REFERENCES

- 457 **Ang, A.F.; Ashaari, Z.; Lee, S.H.; Tahir, P.M.; Halis, R. 2019.** Lignin-based
458 copolymer adhesives for composite wood panels—A review. *Int J Adhes Adhes* 95:
459 102408. <https://doi.org/10.1016/j.ijadhadh.2019.102408>
- 460 **ASA American Soybean Association 2020.** *Soy stats Report*. United States.
461 https://soygrowers.com/wp-content/uploads/2020/05/SoyStats2020_for-WEB.pdf

- 462 **Aydin, I.; Colakoglu, G. 2007.** Variation in surface roughness, wettability and some
463 plywood properties after preservative treatment with boron compounds. *Build Environ*
464 42(11): 3837-3840. <https://doi.org/10.1016/j.buildenv.2006.11.009>
- 465 **Boehme, C.; Hora, G. 1996.** Water absorption and contact angle measurement of native
466 European, North American and tropical wood species to predict gluing
467 properties. *Holzforschung* 50(3): 269-276. <https://doi.org/10.1515/hfsg.1996.50.3.269>
- 468 **Buddi, T.; Mahesh, K.; Muttill, N.; Rao, B.N.; Nagalakshmi, J.; Singh, S.K. 2017.**
469 Characterization of plywoods produced by various bio-adhesives. *Mater Today* 4(2):
470 496-508. <https://doi.org/10.1016/j.matpr.2017.01.050>
- 471 **Bulfe, N.M. L; Fernández, M.E. 2017.** Anatomía funcional del leño juvenil de *Pinus*
472 *taeda* L: variabilidad genotípica y plasticidad anatómica ante déficit hídrico. *Revista de*
473 *la Facultad de Agronomía, La Plata* 116(2): 225-240.
474 <https://revistas.unlp.edu.ar/revagro/article/view/6177>
- 475 **Calvo, C.F.; Cotrina, A.; Cuffré, A.G.; Piter, J.; Stefani, P.M.; Torrán, E.A. 2006.**
476 Variación radial y axial del hinchamiento, del factor anisotrópico y de la densidad, en el
477 *Eucalyptus grandis* de Argentina. *Maderas-Cienc Tecnol* 8(3):159-168.
478 <http://dx.doi.org/10.4067/S0718-221X2006000300003>
- 479 **Ciannamea, E.; Martucci, J.; Stefani, P.; Ruseckaite, R. 2012.** Bonding Quality of
480 Chemically-Modified Soybean Protein Concentrate-Based Adhesives in Particleboards
481 from Rice Husks. *J Am Oil Chem Soc* 89(9): 1733-1741. [https://doi.org/10.1007/s11746-](https://doi.org/10.1007/s11746-012-2058-2)
482 [012-2058-2](https://doi.org/10.1007/s11746-012-2058-2)
- 483 **Ciannamea, E.M.; Marin, D.; Ruseckaite, R.A.; Stefani, P. M. 2017.** Particleboard
484 Based on Rice Husk: Effect of Binder Content and Processing Conditions. *J Renew Mater*
485 5(5): 357-362. <https://doi.org/10.7569/JRM.2017.634125>

- 486 **Ciannamea, E.M.; Stefani, P.M.; Ruseckaite, R.A. 2010.** Medium-density
487 particleboards from modified rice husks and soybean protein concentrate-based
488 adhesives. *Bioresour Technol* 101(2): 818-825.
489 <https://doi.org/10.1016/j.biortech.2009.08.084>
- 490 **Chalapud, M.C.; Herdt, M.; Nicolao, E. S.; Ruseckaite, R.A.; Ciannamea, E.M.;**
491 **Stefani, P.M. 2020.** Biobased particleboards based on rice husk and soy proteins: Effect
492 of the impregnation with tung oil on the physical and mechanical behavior.
493 *Constr Build Mater* 230: 116996. <https://doi.org/10.1016/j.conbuildmat.2019.116996>
- 494 **Chandler, J.G.; Brandon, R.L.; Frihart, C.R . 2005.** Examination of adhesive
495 penetration in modified wood using fluorescence microscopy. *ASCSpring 2005*
496 *Convention and Exposition: April 17-20, Columbus, OH.*[Bethesda, Md.: Adhesive and
497 Sealant Council, 2005]: 10 p. <https://www.fs.usda.gov/treearch/pubs/23115>
- 498 **Denne, M. P. 1989.** Definition of latewood according to Mork (1928). *IAWA J* 10(1):
499 59-62. <https://doi.org/10.1163/22941932-90001112>
- 500 **FAOSTAT 2018.** Food and Agriculture Organization of the United Nations. Rome, Italy.
501 <http://www.fao.org/faostat>
- 502 **Frihart, C.R. 2005.** Adhesive bonding and performance testing of bonded wood
503 products. In *Advances in Adhesives, Adhesion Science, and Testing*. Damico, D. (ed.),
504 West Conshohocken, PA: USA. ASTM International. 1-12.
505 <https://doi.org/10.1520/STP11654S>
- 506 **Frihart, C.R.; Hunt, C.G. 2010.** *Wood handbook: wood as an engineering material*.
507 Centennial ed. General technical report FPL; GTR-190. Madison, WI: US Dept. of
508 Agriculture, Forest Service, Forest Products Laboratory.
509 https://www.fpl.fs.fed.us/documnts/fplgtr/fpl_gtr190.pdf

- 510 **Frihart, C.R.; Birkeland, M.J. 2014.** Soy properties and soy wood adhesives. *Soy based*
511 *chemicals and materials. J Am Chem Soc* <https://doi.org/10.1021/bk-2014-1178.ch008>
- 512 **Ghahri, S.; Chen, X.; Pizzi, A., Hajihassani, R.; Papadopoulos, A.N. 2021.** Natural
513 Tannins as New Cross-Linking Materials for Soy-Based Adhesives. *Polymers* 13(4): 595.
514 <https://doi.org/10.3390/polym13040595>
- 515 **Goche Télles, J.R.; Velázquez Martínez, A.; Borja de la Rosa, A.; Capulín Grande,**
516 **J.; Palacios Mendoza, C. 2011.** Variación radial de la densidad básica en *Pinus patula*
517 Schltdl. et Cham. de tres localidades en Hidalgo. *Rev Mex Cienc Forestales* 2(7): 71-78.
518 [http://www.scielo.org.mx/scielo.php?script=sci_arttext&pid=S2007-](http://www.scielo.org.mx/scielo.php?script=sci_arttext&pid=S2007-11322011000500006)
519 [11322011000500006](http://www.scielo.org.mx/scielo.php?script=sci_arttext&pid=S2007-11322011000500006)
- 520 **Hunt, C.G.; Frihart, C.R.; Dunky, M.; Rohumaa, A. 2018.** Understanding wood
521 bonds—going beyond what meets the eye: a critical review. *RAA* 6(4): 369-440.
522 <https://doi:10.7569/RAA.2018.097312>
- 523 **Instituto argentino de normalización y certificación. 2006.** Norma IRAM 9562:2006:
524 Determinación de la calidad de encolado. Buenos Aires, Argentina.
- 525 **Instituto Argentino De Normalización y certificación. 1963.** Norma IRAM 9532:
526 Método de determinación de la humedad. Buenos Aires. Argentina.
- 527 **Instituto Argentino De Normalización y certificación. 1973.** Norma IRAM 9544:
528 Método de determinación de la densidad aparente. Buenos Aires. Argentina.
- 529 **Jakes, J.E.; Frihart, C.R.; Hunt, C.G.; Yelle, D J.; Plaza, N.Z.; Lorenz, L.; Grigsby,**
530 **W.; Ching, D.J.; Kamke, F.; Gleber, S.C. 2019.** X-ray methods to observe and quantify
531 adhesive penetration into wood. *J Mater Sci* 54(1): 705-718.
532 <https://doi.org/10.1007/s10853-018-2783-5>
- 533 **Kamke, F.A.; Lee, J.N. 2007.** Adhesive penetration in wood—a review. *Wood Fiber Sci*
534 39(2): 205-220. <https://wfs.swst.org/index.php/wfs/article/view/641>

- 535 **Kumar, R.; Choudhary, V; Mishra, S.; Varma I.K.; Mattiason, B. 2002.** Adhesives
536 and plastics based on soy protein products. *Ind Crop Prod* 16(3): 155-172.
537 [https://doi.org/10.1016/S0926-6690\(02\)00007-9](https://doi.org/10.1016/S0926-6690(02)00007-9)
- 538 **Liu, Y.; Li, K. 2002.** Chemical modification of soy protein for wood adhesives.
539 *Macromol Rapid Commun* 23(13): 739-742. [https://doi.org/10.1002/1521-3927\(20020901\)23:13<739::AID-MARC739>3.0.CO;2-0](https://doi.org/10.1002/1521-3927(20020901)23:13<739::AID-MARC739>3.0.CO;2-0)
- 541 **Marra, A.A., 1992.** *Technology of wood bonding: principles in practice.* Van Nostrand.
542 New York, United States.
- 543 **Mo, X.; Sun, X.S. 2013.** Soy proteins as plywood adhesives: formulation and
544 characterization. *J Adhes Sci Technol* 27(18-19): 2014-2026.
545 <https://doi.org/10.1080/01694243.2012.696916>
- 546 **Monteoliva, S.; Barotto, A.J.; Fernandez, M.E. 2015.** Anatomía y densidad de la
547 madera en *Eucalyptus*: variación interespecifica e implicancia en la resistencia al estrés
548 abiótico. *Rev Fac Agro* 114(2): 209-217.
549 <http://revista.agro.unlp.edu.ar/index.php/revagro/article/view/130>
- 550 **Nicolao, E.; Leiva, P.; Chalapud, M.; Ruseckaite, R.; Ciannamea, E.; Stefani, P.**
551 **2020.** Flexural and tensile properties of biobased rice husk-jute-soybean protein
552 particleboards. *J Build Eng* 101261. <https://doi.org/10.1016/j.jobe.2020.101261>
- 553 **Nordqvist, P.; Nordgren, N.; Khabbaz, F.; Malmström, E. 2013.** Plant proteins as
554 wood adhesives: Bonding performance at the macro-and nanoscale. *Ind Crops Prod* 44:
555 246-252. <https://doi.org/10.1016/j.indcrop.2012.11.021>
- 556 **Oliveira de, R.G.; Gonçalves, F.G.; Segundinho, P.G. de A.; Oliveira, J.T. da S.;**
557 **Paes, J. B; Chaves, I.L.; Brito, A.S. 2020.** Analysis of glue line and correlations
558 between density and anatomical characteristics of *Eucalyptus grandis* × *Eucalyptus*

- 559 *urophylla* glulam. *Maderas-Cienc Tecnol* 22(4): 495-504.
560 <http://dx.doi.org/10.4067/S0718-221X2020005000408>
- 561 **Palacios Mendoza, C. 2011.** Variación radial de la densidad básica en *Pinus patula*
562 Schlttdl. et Cham. de tres localidades en Hidalgo. *Rev Mex Cienc Agric* 2(7): 71-78.
563 <http://www.scielo.org.mx/scielo.php?pid=S2007->
564 [11322011000500006&script=sci_arttext](http://www.scielo.org.mx/scielo.php?pid=S2007-11322011000500006&script=sci_arttext)
- 565 **Papp, E.A.; Csiha, C. 2017.** Contact angle as function of surface roughness of different
566 wood species. *Surf Interfaces* 8: 54-59. <https://doi.org/10.1016/j.surfin.2017.04.009>
- 567 **Piter, J.; Cotrina A.; Zitto, M.S.; Stefani, P.M.; Torrán, E. 2007.** Determination of
568 characteristic strength and stiffness values in glued laminated beams of Argentinean
569 *Eucalyptus grandis* according to European standards. *Holz Roh Werkst* 65(4): 261-266.
570 <https://doi.org/10.1007/s00107-006-0161-5>
- 571 **Pizzi, A. 2006.** Recent developments in eco-efficient bio-based adhesives for wood
572 bonding: opportunities and issues. *J Adhes Sci Technol* 20(8): 829-846.
573 <https://doi.org/10.1163/156856106777638635>
- 574 **Plinke, B. 2002.** Automatic determination of wood fibre failure percentage of plywood
575 shear samples Wood based materials. In Wood composites and chemistry : International
576 symposium, September 19-20, 2002. Vienna, Austria Wien, pp.247-256
577 <http://publica.fraunhofer.de/documents/N-15521.html>
- 578
579 **Rohumaa, A.; Hunt, C.G.; Hughes, M., Frihart, C.R., Logren, J. 2013.** The influence
580 of lathe check depth and orientation on the bond quality of phenol-formaldehyde-bonded
581 birch plywood. *Holzforschung* 67(7): 779-786. <https://doi.org/10.3390/polym13040595>
- 582 **Rowell, R.M. 2012.** *Handbook of wood chemistry and wood composites*. CRC press.
583 United States.

- 584 **Salthammer, T.; Mentese, S.; Marutzky, R. 2010.** Formaldehyde in the indoor
585 environment. *Chem Rev* 110(4): 2536-2572. <https://doi.org/10.1021/cr800399g>
- 586 **Sánchez Acosta, M.; Zakowicz, N.; Harrand, L.; Cuffre, A.; Torran, E.; Calvo P.J.**
587 **2005.** Propiedades físico mecánicas de la madera de *Eucalyptus grandis* de las
588 procedencias genéticas: Kendall (Australia), Huerto semillero de Sudáfrica y semilla
589 local Concordia, plantadas comercialmente en Argentina. In *Congreso Mundial IUFRO.*
590 Entre Rios, Argentina.
- 591 **Scheikl, M.; Dunky, M. 1998.** Measurement of dynamic and static contact angles on
592 wood for the determination of its surface tension and the penetration of liquids into the
593 wood surface. *Holzforschung* 52(1): 89-94. <https://doi.org/10.1515/hfsg.1998.52.1.89>
- 594 **Stefani, P.M.; Peña C.; Ruseckaite, R.A.; Piter, J.; Mondragon, I. 2008.** Processing
595 conditions analysis of *Eucalyptus globulus* plywood bonded with resol-tannin adhesives.
596 *Bioresour Technol* 99(13): 5977-5980. <https://doi.org/10.1016/j.biortech.2007.10.013>
- 597 **Vázquez, G.; Galinanes, C.; Freire, M.S.; Antorrena, G.; González-Alvarez, J. 2011.**
598 Wettability study and surface characterization by confocal laser scanning microscopy of
599 rotary-peeled wood veneers. *Maderas-Cienc Tecnol* 13(2): 183-192.
600 <https://doi.org/10.4067/S0718-221X2011000200006>
- 601 **Wang, F.; Wang, J.; Chu, F.; Wang, C.; Jin, C.; Wang, S.; Pang, J. 2018.**
602 Combinations of soy protein and polyacrylate emulsions as wood adhesives. *Int J Adhes*
603 *Adhes* 82: 160-165. <https://doi.org/10.1016/j.ijadhadh.2018.01.002>
- 604 **Wolkenhauer, A.; Avramidis, G.; Hauswald, E.; Militz, H.; Viöl, W. 2009.** Sanding
605 vs. plasma treatment of aged wood: A comparison with respect to surface energy. *Int J*
606 *Adhes Adhes* 29(1): 18-22. <https://doi.org/10.1016/j.ijadhadh.2007.11.001>
- 607 **Xi, X.; Pizzi, A.; Frihart, C.; Lorenz, L.; Gerardin, C. 2020.** Tannin plywood
608 bioadhesives with non-volatile aldehydes generation by specific oxidation of mono-and

609 disaccharides. *Int J Adhes Adhes* 98: 102499.

610 <https://doi.org/10.1016/j.ijadhadh.2019.102499>

Accepted manuscript